

Supplementary Information

Engineering Robust Metal–Phenolic Network Membranes for Uranium Extraction from Seawater

Wei Luo^{1,2}, Gao Xiao^{3,4}, Fan Tian⁵, Joseph J. Richardson⁶, Yaping Wang^{1,2}, Jianfei Zhou^{1,2},
Junling Guo^{1,2,3*}, Xuepin Liao^{1,2*}, Bi Shi^{1,2}

¹Department of Biomass and Leather Engineering, Sichuan University, Chengdu, Sichuan 610065, China. E-mail: xpliao@scu.edu.cn.

²National Engineering Laboratory for Clean Technology of Leather Manufacture, Sichuan University, Chengdu, Sichuan 610065, China.

³Wyss Institute for Biologically Inspired Engineering, Harvard University, Boston, Massachusetts 02115, United States. E-mail: junling.guo@wyss.harvard.edu.

⁴College of Environment and Resources, Fuzhou University, Fuzhou, Fujian 350108, China.

⁵Department of Applied Mathematics and Statistics, Johns Hopkins University, Baltimore, Maryland 21287, United States.

⁶Department of Chemical and Biomolecular Engineering, The University of Melbourne, Parkville, Victoria 3010, Australia.

*Correspondence to: Junling Guo (E-mail: junling.guo@wyss.harvard.edu); Xuepin Liao (E-mail: xpliao@scu.edu.cn).

Table of Contents

Section 1. General Materials.....	3
Section 2. Characterization	3
Section 3. Polyphenol-Based Functionalization of Microporous Membrane.....	3
Section 4. Uranium Adsorption Kinetics on MPN-Based Membrane.....	3
Section 5. Continuous Extraction of Uranium.....	4
Section 6. Anti-Fouling Testing.....	5
Section 7. Uranium Extraction Experiments in Artificial Seawater	5
Section 8. Marine-Field Test of Uranium Extraction from Seawater.....	7
Section 9. Supplementary Tables S1-S2 and Figures S1-S17	8
Section 10. Supplementary References.....	27

Section 1. General Materials

Microporous polyamide membranes (surface porosity = 70%, average pore size 4.5 μm , membrane thickness = 146 μm) were acquired from Shanghai Xinya instruments Co., Ltd (China). Uranyl nitrate hexahydrate ($\text{UO}_2(\text{NO}_3)\cdot 6\text{H}_2\text{O}$) was obtained from Hubei Chu shengwei Chemical Co., Ltd (China). *Acacia mearnsii* tannin (polyphenols) was friendly provided by Dymatic Chemicals, Inc (China). NaHCO_3 , MgCl_2 , CaCl_2 , CuSO_4 , NaCl , glutaraldehyde, and other metal salts were all analytical grade and presented by Chengdu Kelong Chemical Reagent Factory (China).

Section 2. Characterization

Field emission scanning electron microscopy (FESEM, S-4800, Hitachi Co., Japan) with an acceleration voltage of 3 kV was used to observe surface morphology of the membrane. Pure water flux of membrane before and after tannin immobilized was determined by membrane filtration system.

Section 3. Polyphenol-Based Functionalization of Microporous Membrane

Polyphenols used in this work were extracted from the barks of *Acacia mearnsii* trees which was provided by Dymatic Chemicals, Inc. The functionalized of polyphenols on polyamide microporous membrane was achieved by our modified reported method.¹ Briefly, polyamide microporous membrane was immersed in 0.5 wt% aqueous *Acacia mearnsii* tannin solution for 15 h to acquire adsorption equilibrium, rinsed by deionized water and then suspended in 10 wt% glutaraldehyde solution at 303 K for 3 h to covalently immobilize tannin on polyamide microporous membrane. After washed thoroughly with deionized water and ethanol, the polyphenol-functionalized membrane was obtained. Metal-phenolic networks, also named as MPN, can be formed on the surface of membrane during the processing of seawater containing uranium².

Section 4. Uranium Adsorption Kinetics on MPN-Based Membrane

4.1. Adsorption isotherm

Adsorption isotherm studies were carried out in 50 mL solutions with initial U(VI) concentration ranging from 0.1 to 2 mmol/L. The pH of the solutions was adjusted to 5.0, and 0.180 g polyphenol-functionalized membrane was suspended in solution, and then the adsorption experiments were conducted with constant stirring for 24 h at 303, 313, 323 and 333 K, respectively. The concentration of U(VI) after adsorption equilibrium attained was analyzed by ICP-OES, and adsorption capacity was calculated according to eqs (1).³

$$q_e = \frac{V(C_0 - C_e)}{m} \quad (1)$$

where C_0 and C_e represent the initial and the equilibrium U(VI) concentration ($\text{mg}\cdot\text{L}^{-1}$), respectively. V is the volume of U(VI) solution (L) and m is the dosage of adsorbent (g).

4.2. Adsorption kinetics

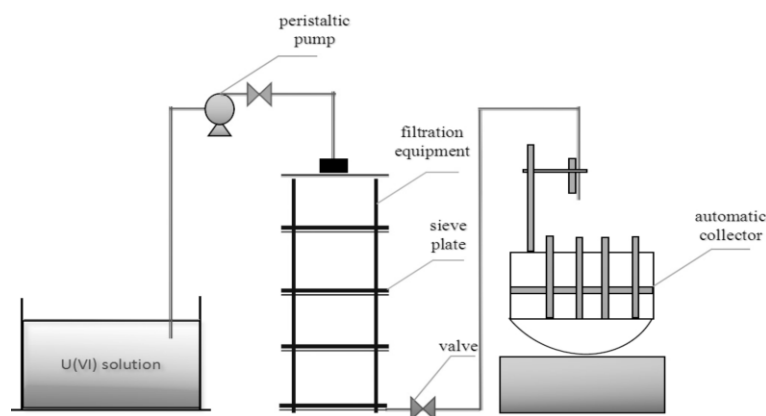
The adsorption procedure was similar with that of adsorption isotherm study, but the concentration of U(VI) was analyzed at a regular interval by ICP-AES during adsorption process. The adsorption capacity at time t (min) was obtained by mass balance calculation and was denoted as q_t (mg/g).

4.3 Influence of coexisted ions

The adsorption procedure was similar with that of adsorption isotherm study. However, the coexisted ions in the U(VI) solution was provided by the addition of Na^+ , Mg^{2+} , Ca^{2+} , Cu^{2+} , Fe^{2+} , Ni^{2+} , V^{5+} , Cl^- , HCO_3^- , and NO_3^- ranging from 0 to 100 mmol/L, respectively.

Section 5. Continuous Extraction of Uranium

Continuous adsorption experiments were performed using membrane filtration system and operated at atmosphere pressure, as shown in **Scheme 1**. Polyphenol-functionalized membrane with diameter of 7.0 cm was fixed on sieve plate, and this membrane filtration system could be equipped with single and/or multilayer membrane. The influence of initial concentration of U(VI) (0.05, 0.1, 0.2, 0.3 and 0.4 mmol/L, pH=5.0) and number of membrane layer on the adsorption performances were investigated at a feeding rate of 20 mL/min.



Scheme 1. The scheme of filtration system based on polyphenol-functionalized

membrane used for adsorption kinetics.

Section 6. Anti-Fouling Testing

The anti-fouling performance and reusability of composite membranes were investigated by U(VI) solution with the concentration of 0.1mmol/L using the similar procedure mentioned above. The U(VI) solution was filtered through composite membrane for total 2 h under 1 Pa, and the permeate flux was tested after certain time intervals (20, 40, 60, 80, 100, and 120 min) for first run. After flushing with 0.1M HNO₃, the permeate flux of cleaned membranes for U(VI) solution was operated for second and third run as outlined above.

Generally, the flux recovery ratio (FRR) and total flux decline ration (FDR) were used to evaluate the antifouling property, which can be expressed by following two equations:⁴

$$FRR = \frac{J_{pi}}{J_{p1}} \times 100\%$$

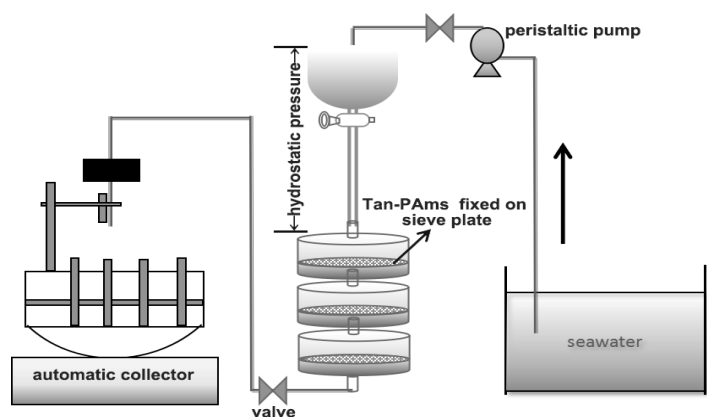
$$FDR = \left(1 - \frac{J_{pi,2}}{J_{p1}} \right) \times 100\%$$

where J_{p1} , J_{pi} and $J_{pi,2}$ represent the permeate flux of composite membrane for first ($i = 1$) run at the beginning, the i run at the beginning, and the i run after 2 h filtration, respectively.

Section 7. Uranium Extraction Experiments in Artificial Seawater

Artificial seawater was formulated according to literature.^{5, 6} Typically, uranyl nitrate ([UO₂(NO₃)₂]) was prepared into 1mg/L solution, then 3.3mL of uranyl nitrate stock solution, 24.53 g of sodium chloride (NaCl), 11.11 g of magnesium chloride (MgCl₂·6H₂O), 4.09g sodium sulfate (Na₂SO₄) and varieties of metal salts including KCl, KBr, CaCl₂ and NaHCO₃ were dissolved in 1 L of deionized water. The element analysis of artificial seawater is shown in Table 1.

Uranium extraction experiments were performed using membrane filtration system and operated at atmosphere pressure, as shown in **Scheme 2**. Polyphenol-functionalized membrane with diameter of 5.0 cm was fixed on sieve plate, and this membrane filtration system could be equipped with single and/or multilayer membrane.



Scheme 2. The scheme of filtration system equipped with multiple polyphenol-functionalized membranes used for artificial and marine-field test. The design of this system was capable of processing long-term and large volume seawater.

The effects of membrane number, flow rate, and coexisted ions on extraction of uranium (VI) were investigated in detail. The analysis of uranium concentration determined by inductively coupled plasma-mass spectroscopy (ICP-MS, NexION 300X). The extraction rate was calculated by the difference of the U(VI) equilibrium concentration before and after extraction (see Eq. (2))

$$\text{Extraction rate} = \frac{C_0 - C_e}{C_0} \times 100\% \quad \text{Eq.(2)}$$

In Eq. (1), C_0 (mg/L) and C_e (mg/L) are the initial concentration and equilibrium concentration of uranium in the solutions, respectively.

Table 1. Elemental analysis for the artificial seawater

Elements	Content (Every litre of seawater)
NaCl	24.53g
MgCl ₂ ·6H ₂ O	11.11g
Na ₂ SO ₄	4.09g
KBr	0.1g
KCl	0.7g
CaCl ₂	1.16g
NaHCO ₃	0.2g
U(VI)	3.3μg

Section 8. Marine-Field Test of Uranium Extraction from Seawater.

In order to evaluate the potential application of polyphenol-functionalized membrane for uranium extraction from seawater, we carried out the experiments on adsorption of uranium (VI) from natural seawater.⁷ The natural seawater used in the adsorption experiments came from near surface seawater from Shangdong Province, China, collected in the tanks. The concentrations of uranium ions in seawater is 3.29 $\mu\text{g/L}$. Figure S12 showed the photo pictures of the location and marine-field test setting.

Section 9. Supplementary Tables S1-S2 and Figures S1-S17

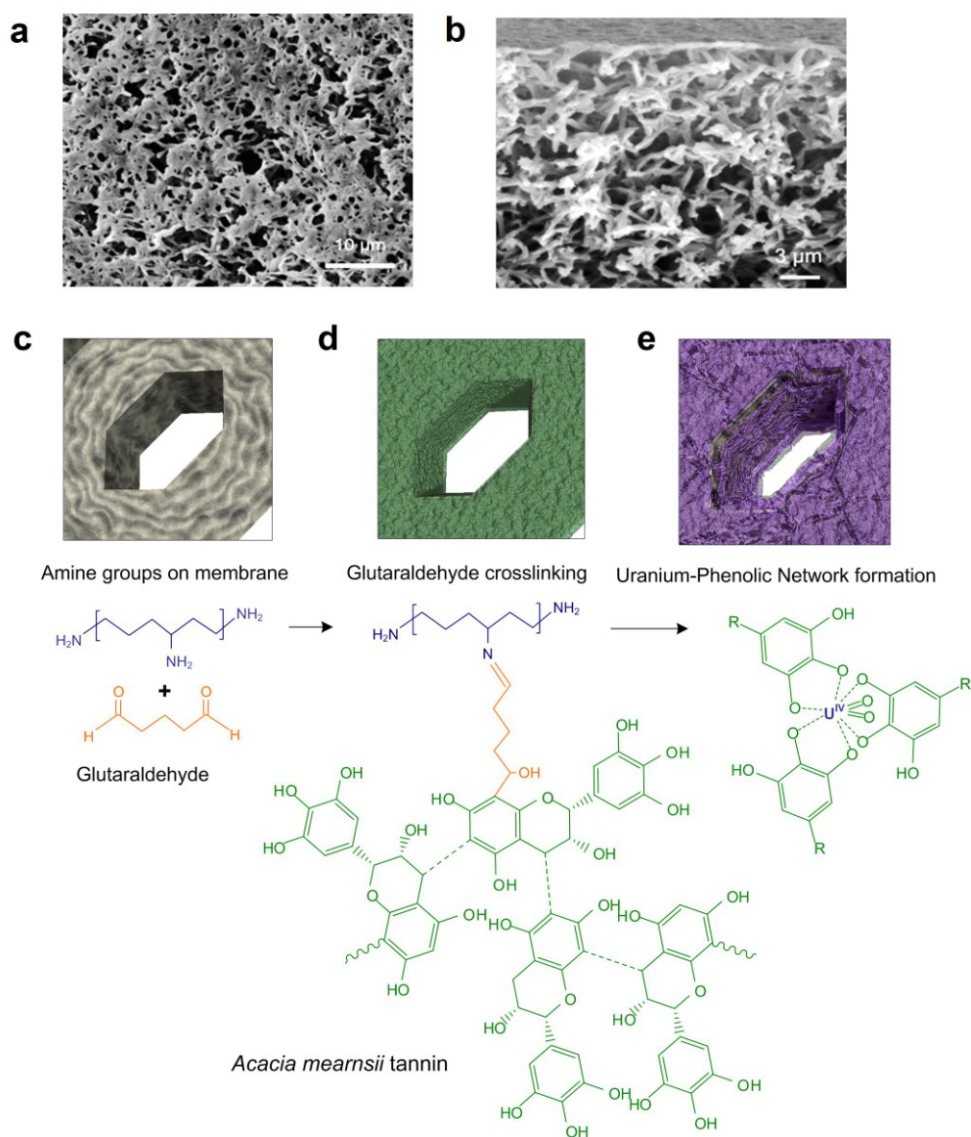


Figure S1. SEM images of the microporous polyamide membrane, (a) the surface of the polyphenol-functionalized membrane, (b) cross-section of the microporous polyamide membrane. (c) The presence of amine groups on the membrane allows for further crosslinking with polyphenols (tannins) through reaction with glutaraldehyde. (d) The polyphenols were first immobilized on the membrane through covalent bonds on the membrane surface. (e) The immobilized polyphenols can coordinate with uranyl species in seawater to form robust and reversible uranium-phenolic networks on the membrane.

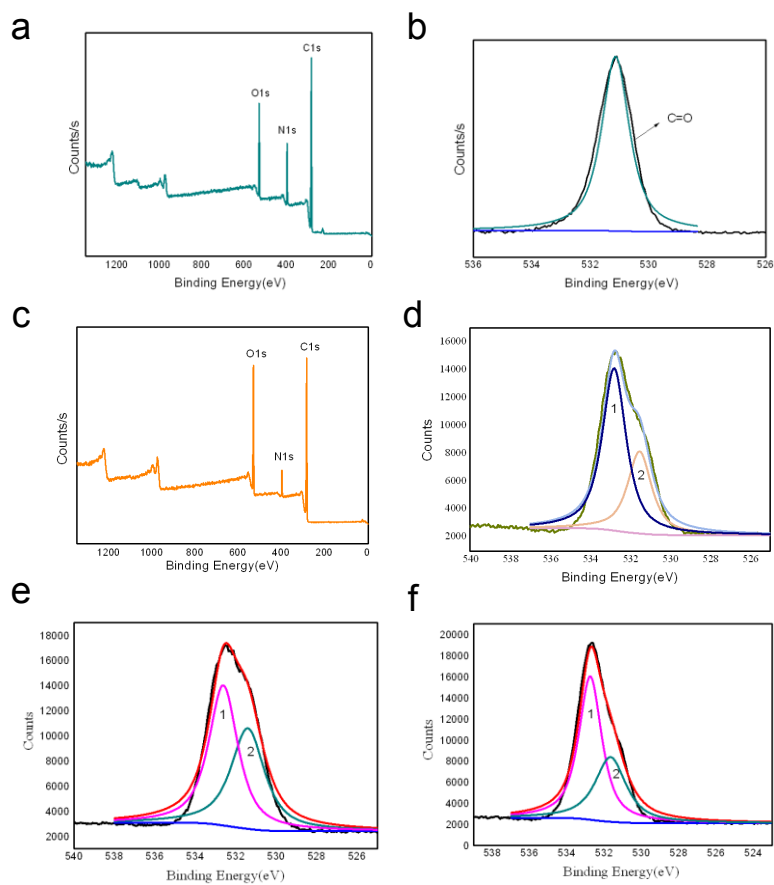


Figure S2. XPS survey spectra of microporous polyamide membrane (a) and polyphenol-functionalized membrane (c) , O_{1s} core level spectra of microporous polyamide membrane (b) and polyphenol-functionalized membrane (d). XPS O_{1s} spectra of the membranes polyphenol-functionalized membrane-U(VI) (e) and polyphenol-functionalized membrane-U(VI) after desorption (f).

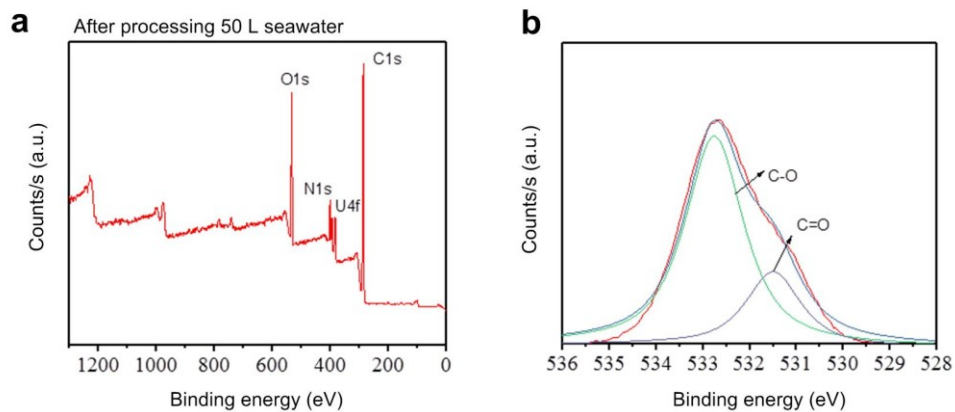


Figure S3. (a) XPS scanning spectrum of the polyphenol-functionalized membrane after processing 50 L seawater. (b) High resolution XPS O_{1s} spectrum of the polyphenol-functionalized membrane after processing 50 L seawater.

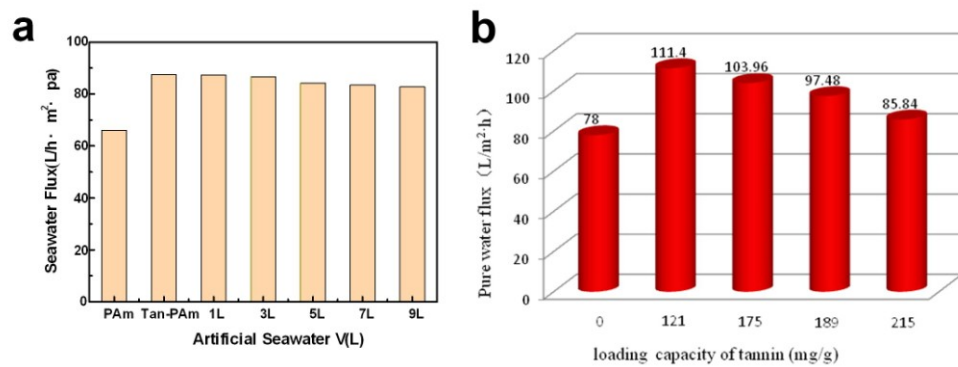


Figure S4. Seawater permeation flux of the polyphenol-functionalized membrane (a), Pure water flux of microporous polyamide membrane and polyphenol-functionalized membrane (b).

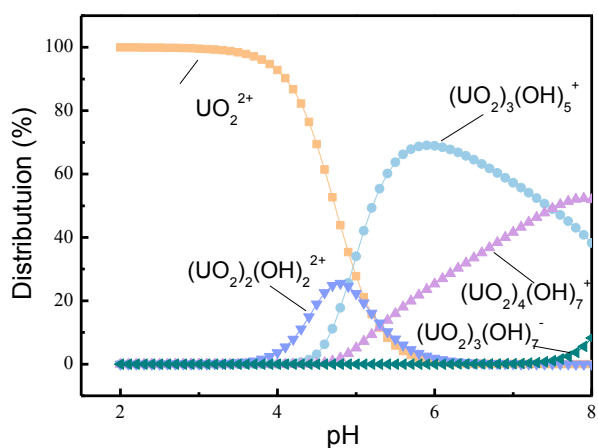


Figure S5. Effect of initial pH on the adsorption capacity of U(VI) on polyphenol-functionalized membrane and distribution of UO_2^{2+} species in aqueous solution at different pHs (calculated by Visual MINEQL, NIST database. Initial conc. of $\text{UO}_2^{2+} = 1.0 \text{ mmol/L}$): initial U(VI) concentration 1 mmol/L, temperature 303 K.

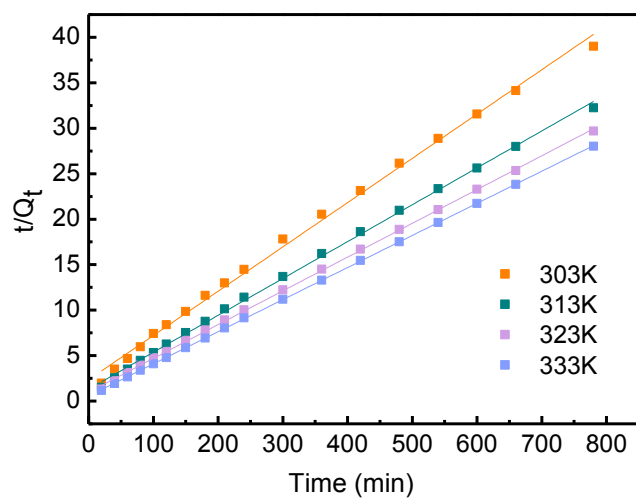


Figure S6. Adsorption kinetics of U(VI) on polyphenol-functionalized membrane: U(VI) concentration 1 mmol/L, pH 5.0, Regression by the pseudo-second-order equation.

Table S1. Fitting parameters of the pseudo-first-order and pseudo-second-order models

temperature (<i>K</i>)	Pseudo-second-order			Pseudo-first-order		
	R^2	k_2	$q_{e,cal}$ (mmol/g)	$q_{e,exp}$ (mmol/g)	R^2	k_1
303	0.9966	0.102	0.205	0.200	0.7717	0.551
313	0.9988	0.124	0.247	0.241	0.7975	0.568
323	0.9996	0.141	0.269	0.263	0.8682	0.662
333	0.9999	0.221	0.283	0.278	0.9607	0.606

$q_{e,exp}$: the maximum adsorption capacity determined by experiments.

$q_{e,cal}$: the maximum adsorption capacity determined by calculation.

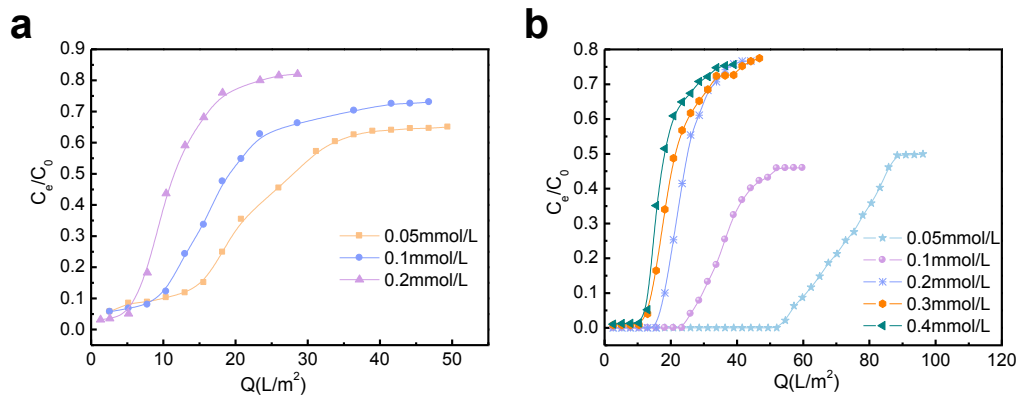


Figure S7. Effect of initial concentration and number of membrane layer on the breakthrough profiles for U(VI) adsorption, (a) Single layer membrane, (b) double layer membranes.

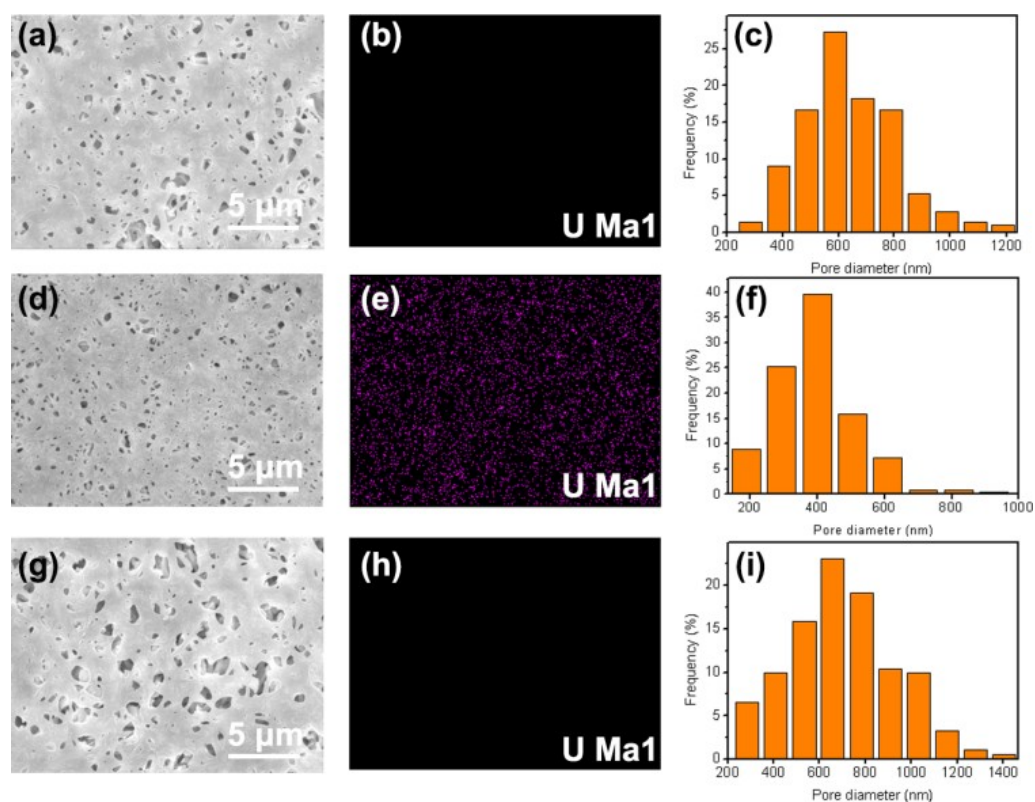


Figure S8. The SEM images, EDX element mapping, and pore-size distribution of the membranes. (a-c) polyphenol-functionalized membrane, (d-f) polyphenol-functionalized membrane U(VI), and (g-i) polyphenol-functionalized membrane U(VI) after desorption.

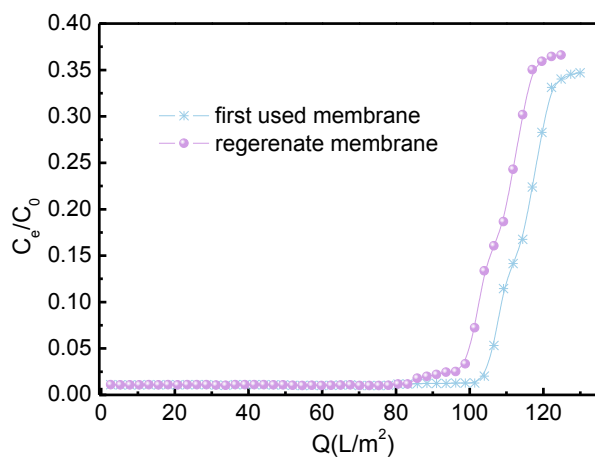


Figure S9. Recycling performance of polyphenol-functionalized membrane on extraction system: U(VI) concentration 0.05 mmol/L, three layer membranes, 0.1M HNO_3 , breakthrough curves of U(VI) on polyphenol-functionalized membrane.

Table S2. Extraction rate of each membrane

	The first layer	The second layer	The third layer
Extraction rate	43%	22%	16%

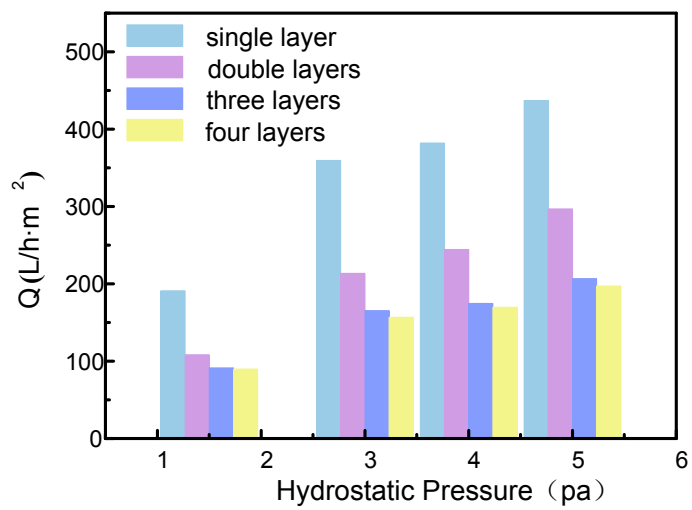


Figure S10. Effect of hydrostatic pressure on seawater flow rate.

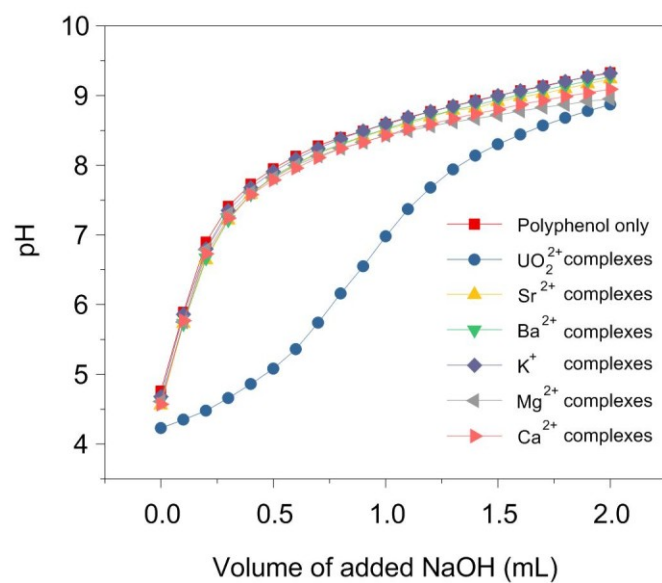


Figure S11. Titration curves of metal-phenolic complexes with different metal ions at room temperature. The lagging pH change of the uranium-phenolic complexes suggested a higher coordination stability.

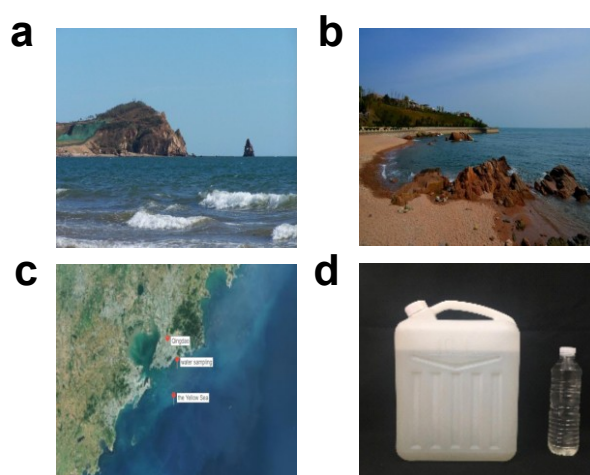


Figure S12. Marine field tests were performed at the Yellow Sea area ($36^{\circ}03'11.3''\text{N}$ $120^{\circ}25'23.7''\text{E}$) as northern part of East China Sea. The concentration of uranium ions in the seawater is detected to be $3.29 \pm 0.134 \mu\text{g/L}$ through inductively coupled plasma optical emission spectrometry (ICP-OES).

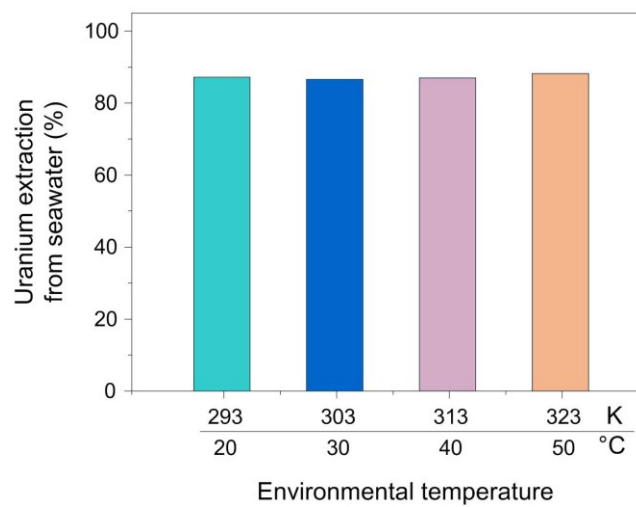


Figure S13. Effect of seawater temperatures on uranium extraction rates based on three layers of MPN-based membranes.

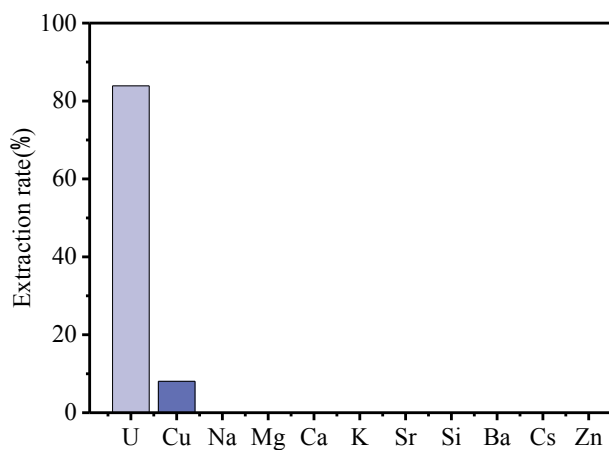


Figure S14. Extraction rates of uranium and other ions after processing 10 L seawater. The concentration of uranium in seawater is only $\sim 3\mu\text{g/L}$, while the concentration of copper is $13.4\ \mu\text{g/L}$, sodium is $10.77\ \text{g/L}$, potassium is $0.399\ \text{g/L}$, magnesium is $1.29\ \text{g/L}$, and calcium is $0.412\ \text{g/L}$. This result shows that the extraction rate of other ions was much smaller than that of uranium, indicating the favorable adsorption affinity for uranium ions in the marine test.

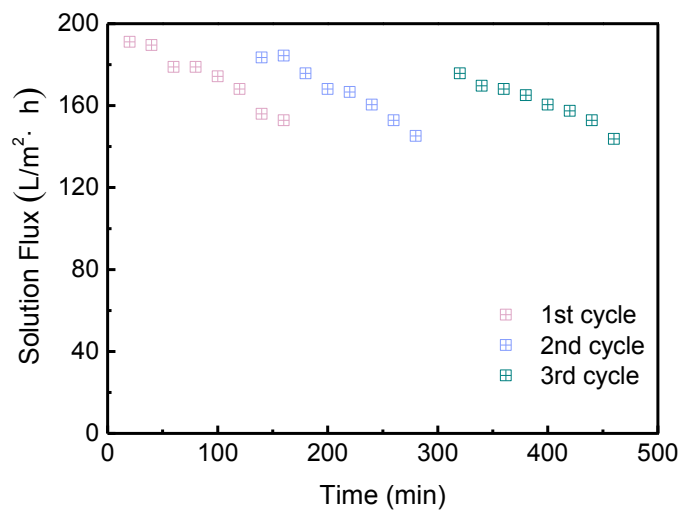


Figure S15. Antifouling property and reusability of membranes: seawater, three layer membranes, 0.1M HNO₃, The time dependence of permeate flux variations

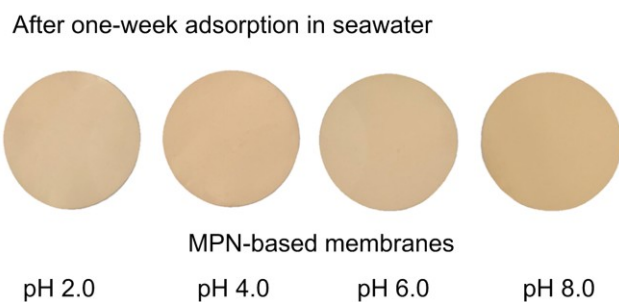


Figure S16. Photographs of MPN-based membranes after one-week adsorption in seawater adjusted to different pH. The seawater was sampled from the Yellow Sea portion (36°03'11.3"N 120°25'23.7"E) of the northern segment of the East China Sea.

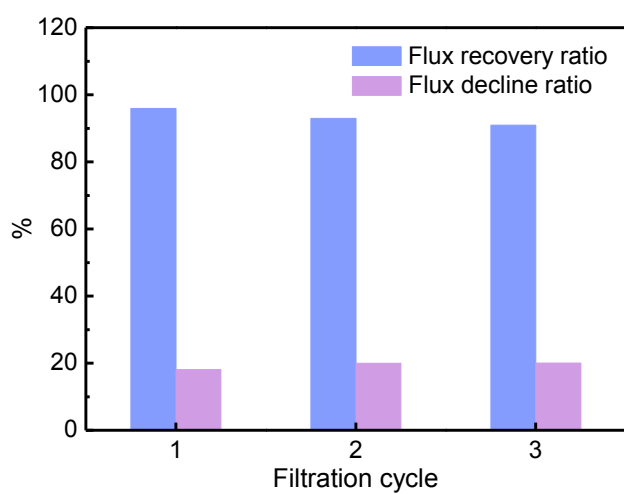


Figure S17. Antifouling property and reusability of membranes: seawater, three layer membranes, 0.1M HNO₃, flux recovery ratio (FRR) and total flux decline ration (FDR).

Section 10. Supplementary References

- 1 X. Liao, Z. Lu, X. Du, X. Liu and B. Shi, *Environ. Sci Tech.*, 2004, **38**, 324.
- 2 J. Guo, Y. Ping, H. Ejima, K. Alt, M. Meissner, J. J. Richardson, Y. Yan, K. Peter, D. von Elverfeldt and C. E. Hagemeyer, *Angew. Chem. Int. Ed.*, 2014, **53**, 5546.
- 3 X. Liao, M. Zhang and B. Shi, *Ind. Eng. Chem. Res.*, 2004, **43**, 2222.
- 4 H. Lee, G. Amy, J. Cho, Y. Yoon, S.-H. Moon and I. S. Kim, *Water Res.*, 2001, **35**, 3301.
- 5 J. R. Kucklick, D. A. Hinckley and T. F. Bidleman, *Marine Chem.*, 1991, **34**, 197.
- 6 K. Saito and T. Miyauchi, *J. Nuclear Sci. Tech.*, 1982, **19**, 145.
- 7 W.-D. Zhai, N. Zheng, C. Huo, Y. Xu, H.-D. Zhao, Y.-W. Li, K.-P. Zang, J.-Y. Wang and X.-M. Xu, *Biogeosciences*, 2014, **11**, 1103.